DESIGN OF A C-BAND COMPACT PHASE SHIFTER FOR PARTICLE ACCELERATORS

Z. Zhang*, Z. Huang, Y. Wei, G. Feng

University of Science and Technology of China, USTC, Hefei, China

Abstract

A phase shifter is a key component to tune the phase of RF power for accelerating or deflecting structures in linear accelerators (linacs). This paper presents the design of a compact C-band variable phase shifter for our high-power test platform. It consists of a dual-polarization mode coupler and a movable short-circuited piston for adjusting RF phases. In order to isolate the coaxial port formed by the movable piston and the pipe a choke is introduced inside the piston. Through optimizations, the RF phase variation is simulated to be 10.1233 °/mm of piston moving distance.

INTRODUCTION

For accelerating structures in linear accelerators (linacs), it is of great importance to satisfy the requirement for precise adjustment of radio frequency (RF) power. The variable RF power splitter is a typical multiport component in high RF power tests, which is used to divide input power proportionally into several branches. In order to distribute RF power among all the output ports not only with arbitrary ratio, but also in high precision, it is necessary to attach a phase shifter to the power splitter to manipulate output RF power [1–4]. There is already a variable phase shifter for X-band implemented in Compact Linear Collider (CLIC) in CERN [5]. To meet the demand for application in C-band linacs, the design of a compact phase shifter at center frequency 5.712 GHz is established in ANSYS HFSS [6]. In this work, the 2-port variable phase shifter realizes the RF phase variation of about 10.12 °/mm of piston moving distance, with the reflection coefficient S_{11} reduced below −55 dB and the transmission coefficient S_{12} achieving nearly 0 dB.

DESIGN AND OPTIMIZATION

The C-band variable phase shifter consists of two components – the E-rotator with dual-polarized modes and the movable short-circuited piston. The input RF power is transmitted through the E-rotator, and excites dual circular-polarized TE_{11} modes in the circular waveguide. Then the RF power enters into the movable piston to be reflected at the terminal short-circuited plane. By adjusting position of the piston, one can alter phase of S_{12} linearly with little power loss through the phase shifter. These two components should be designed and optimized independently from each other.

* zhangzs24231@mail.ustc.edu.cn

E-rotator with Dual-Polarized Modes

The E-rotator is introduced as the power feeding section for the whole phase shifter. The prototype of E-rotator comes from the E-bend 3dB-hybrid, as shown in Fig. 1. The hybrid outputs RF power through port 3 and 4 and the amplitude of each branch is equal to half of the total input power while port 2 is isolated from the other ports. If port 3 and 4 merge into one single circular port on the top of the hybrid, the E-rotator with dual-polarized modes based on the 3dB-hybrid is formed, as shown in Fig. 2.

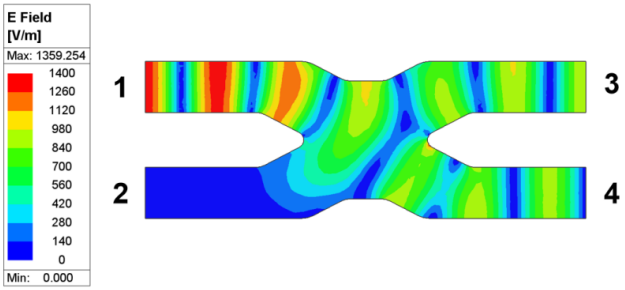

Figure 1: The electric field distribution for an E-hybrid.

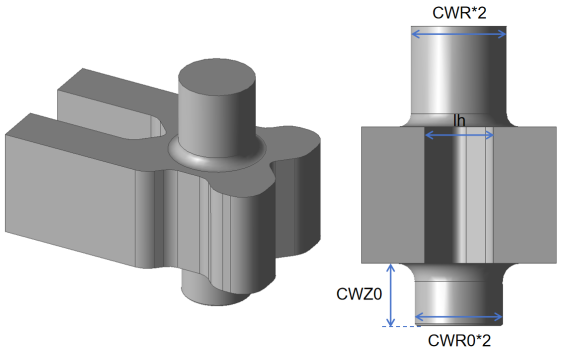

Figure 2: Geometry of the E-rotator with dual-polarized modes.

For the E-rotator, port 3 and 4 of the 3dB-hybrid are short-circuited, and RF power can only be output through the circular waveport, where the movable piston is linked to the rotator. In this case, the original 4-port structure is modified to 3-port structure. It is expected that the input RF power should be transmitted to the circular waveport to be fully adjusted later by the movable piston. As for geometrical dimensions of the component, the model BJ-48 are selected for rectangular waveguide to transmit TE_{10}. The radius of

the circular waveguide is also determined to make sure there are only TE_{11} modes. The bend part near the input rectangular waveguide causes reflection due to the nonconformity of transmission structure. Therefore, the bend functions as an impedance matching section. As for the circular waveguide added on the bottom as well as the terminal short-circuited structure at the far side from the input port, the fields distribution of microwave is optimized to a more symmetric situation, which puts a substantial effect on transmission coefficient S_{13} and isolation S_{12}. Because of orthogonally dual-polarized modes in the circular waveguide, the circular waveport should be treated as two ports (3:1) and (3:2), with each mode seen as single port. Then the E-rotator is treated as a 4-port component. There are four crucial coefficients for performance evaluation — reflection S_{11}, isolation S_{12}, transmission S(1, 3:1) and S(1, 3:2). Since nearly 20 parameters need to be optimized, it is inefficient to respectively analyze all the coefficients. Alexej integrated S(1, 3:1) and S(1, 3:2) and proposed a new goal function for optimization named *FMX*, the formula expressed in Eq.((1)) and [5]:

$$\begin{aligned} FMX = \; & 0.5 - |re[S(1,\,3:1)] \cdot im[S(1,\,3:2)] \\ & - re[S(1,\,3:2)] \cdot im[S(1,\,3:1)]| \\ = \; & 0.5 - |S(1,\,3:1)\; S(1,\,3:2)||\sin\varphi|. \end{aligned} \tag{1}$$

The variation $\varphi = |arg[S(1,\,3:1)] - arg[S(1,\,3:2)]|$. The ideal value of *FMX* is lower than −95 dB. From Eq.(1) one can be easily informed that the following conditions should be satisfied when *FMX* obtains its minimum:

1) $|S(1,\,3:1)|^2 = |S(1,\,3:2)|^2 = 0.5$;

2) $|arg[S(1,\,3:1)] - arg[S(1,\,3:2)]| = 90^\circ + n\pi$.

Condition 1) corresponds to the situation where all the input power is divided equally between two dual-polarized TE_{11} modes. Condition 2) means two dual-polarized TE_{11} modes are strictly orthogonal. Through *FMX*, S(1, 3:1) and S(1, 3:2) are combined into one indicator to reduce complexity of optimization.

Movable Short-Circuited Piston

The movable short-circuited piston is a symmetric structure mainly composed of circular waveguide, as shown in Fig. 3a. The transition whose radius is widen gradually links the circular waveport of the E-rotator and the terminal piston containing short-circuited plane. Given that the reflection coefficient in the short-circuited plane is –1 and the backward wave can be expressed as $e^{j\theta}$ (amplitude of the wave is normalized), the phase of S_{11} in the plane of input port can be written as $\theta = 2\beta\Delta z = (4\pi/\lambda)\Delta z$. The phase can be changed by mechanically changing shortL which is distance between the short-circuited plane and the end of the piston.

In order to operate the piston smoothly, the gap between the movable piston and the inner wall of the circular waveport

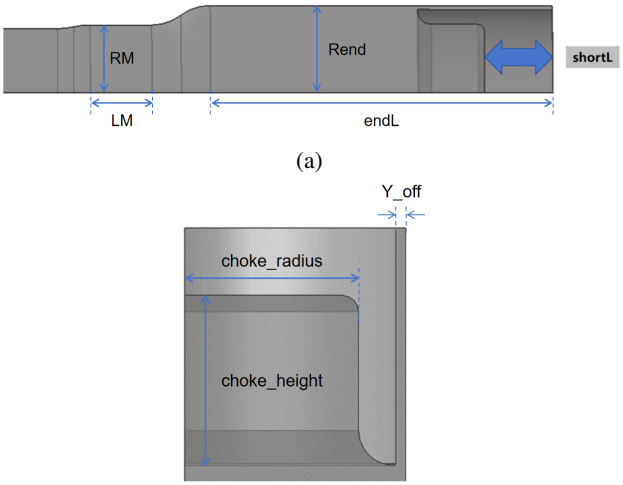

Figure 3: Movable short-circuited piston: (a) geometry (cut view) and (b) choke (cut view).

is left, which inevitably introduces the coaxial port inside the piston. A choke is applied at the terminal to enhance isolation of the coaxial port, as shown in Fig. 3b.

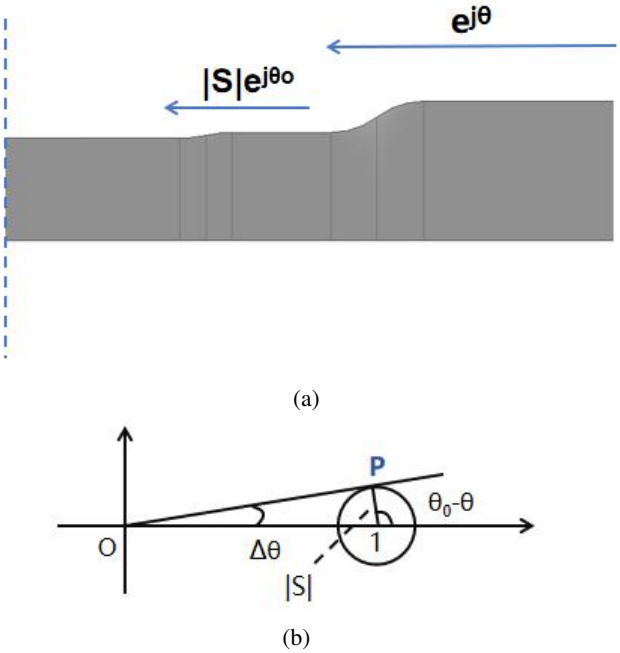

Figure 4: The transition section of the movable short-circuited piston: (a) schematic structure and (b) geometrical representation of phase variation.

However, the transition causes unexpected reflection leading to significant deterioration in the precision of phase variation. This process can be demonstrated by Fig. 4a. In order to figure out how the reflection from the transition influences precision of phase tuning, one can express the reflected wave in Eq.((2)) in the plane of reference where the reflected RF power returns to the E-rotator:

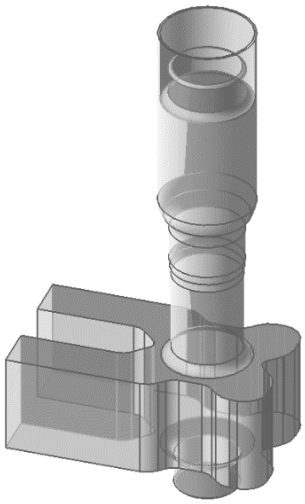

Figure 5: Geometry of the Variable phase shifter.

$$|S|e^{j\theta_0} + e^{j\theta} = e^{j\theta}[1 + |S|e^{j(\theta_0-\theta)}]. \quad (2)$$

The reflected wave can be seen as $e^{j\theta}$, where the amplitude is close to but actually lower than 1. The reflection caused by the transition is expressed as $|S|e^{j\theta_0}$, where the amplitude $|S|$ is approximate to 0 but cannot be ignored, and θ_0 is the initial reference phase. The term inside the square brackets of Eq. (2) can be represented geometrically in Fig. 4b. Phase deviation $\Delta\theta$ always exists if $|S|$ does not equal to zero. When the piston position is shifted the overall phase of S_{11} is $\theta + \Delta\theta$ instead of simply θ, reducing linearity of curve of the phase variation. The higher value of $|S|$, the worse the linearity of phase variation. Based on the analysis above, one can confirm the target of optimization for the piston, which is the restraint of coaxial port isolation S_{12} and the reflection from the transition $|S|$.

RESULTS OF OPTIMIZATION

As shown in Fig. 5, the variable phase shifter is formed by connecting the movable short-circuited piston to the circular waveport of the E-rotator after these two components finish optimization separately. Within the range of the piston position (shortL), S_{11} is less than −58 dB on average, and S_{12} is close to 0 dB, as shown in Fig. 6. The slope of S_{12} fitting phase curve is approximate to 10.1233 °/mm, establishing an optimal precision of phase adjustment. Several main dimensions of the phase shifter are summarized in Table 1.

CONCLUSION

A C-band compact variable phase shifter with high precision of phase variation has been designed in this paper. The phase shifter is composed of the E-rotator with dual-polarized modes and the movable short-circuited piston which are optimized separately. The integrated phase shifter achieves a good linearity with the phase variation precision of 10.1233 °/mm. The reflection coefficient at the input port

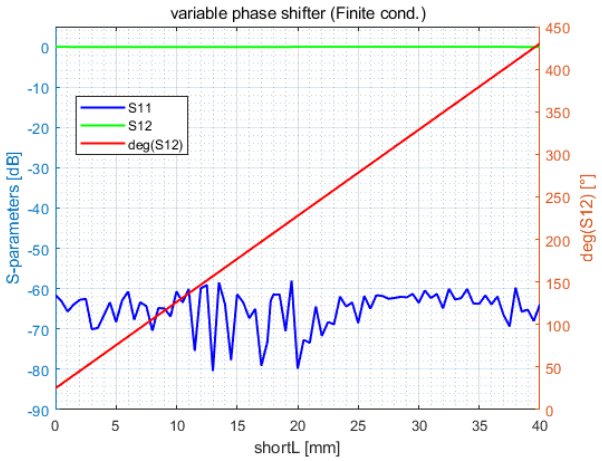

Figure 6: S-parameters of the variable phase shifter.

Table 1: Dimensions of the variable phase shifter

Dimension	Value[mm]
CWR	16.74
CWR0	15.4
CWZ0	21.6
lh	23.88
Rend	22.8
endL	95
RM	17.66
LM	29
choke_radius	17.95
choke_height	17.65
Y_off	1

of the phase shifter is also optimized to be < −50 dB. Therefore, this phase shifter absolutely satisfies the demand for our C-band high-power test platform.

ACKNOWLEDGMENT

This work was supported in part by the "Hundred Talents Program" of Chinese Academy of Sciences (Grant No. KJ2310007003) in part by the Fundamental Research Funds for the Central Universities (Grant No. WK2310000114); in part by Chinese Academy of Sciences President's International Fellowship Initiative (Grant No. 2025PD0102).

REFERENCES

[1] H. Zha *et al.*, "Design of a variable X-band RF power splitter", *Nucl. Instrum. Methods Phys. Res. A*, vol. 859, pp. 47–51, 2017. doi:10.1016/j.nima.2017.04.006

[2] V. D. P. Romano *et al.*, "High power conditioning of X-band variable power splitter and phase shifter", in *Proc. IPAC'19*, Melbourne, Australia, May 2019, pp. 2964–2967. doi:10.18429/JACoW-IPAC2019-WEPRB064

[3] Z. Li *et al.*, "Radio frequency design of a new C-band variable power splitter", *Nucl. Sci. Tech.*, vol. 30, no. 6, p. 100, 2019. doi:10.1007/s41365-019-0611-5

[4] F. Liu *et al.*, "Development of a compact X-band variable-ratio RF power splitter", *Nucl. Instrum. Methods Phys. Res. A*, vol. 1015, p. 165759, 2021. doi:10.1016/j.nima.2021.165759

[5] A. Grudiev, "Design of compact high power RF components at X-band", CERN, Geneva, Switzerland, Rep. CERN-ACC-NOTE-2016-0044, May 2016.

[6] Ansys, *HFSS*. https://www.ansys.com